

# Monte-Carlo-Based Impulse Response Modeling for Underwater Wireless Optical Communication

Feibiao Dong\*, Limei Xu, Dagang Jiang, and Tianhong Zhang

**Abstract**—In underwater wireless optical communication links, the suspended particles in the water can lead to multiple path transmission of the light, causing the temporal dispersion and attenuation of beam pulse. The scattering phase function is a key parameter to model angle scattering in the Monte Carlo simulation and can be approximated by the commonly used Henyey-Greenstein (HG) phase function, but in turbid sea water environment, the HG phase function cannot match well with the measured value of the particle phase function. In this work, instead of using the HG phase function, we make use of the Petzold's measured data value of the scattering phase function in turbid sea water. We propose a numerical solution for the computing of the scattering angle based on the measured particle phase function and present the difference of effect on temporal dispersion between the measurement and HG phase function. Numerical results show that our model is more accurate than the widely used HG model. An analytic double Gamma function is used to fit the Monte Carlo simulation results, and a good fit is found between the double Gamma function and the Monte Carlo simulations.

## 1. INTRODUCTION

Over the past decades, the underwater wireless optical communication sensor network technology has been well developed [1–3] and thus provides a new technique for the ocean detection. The underwater wireless optical communication (UWOC) is a difficult task, due to the high absorption and scattering undergone by the laser beam. Several prior works have focused on the effects of energy loss and transmission direction changing for the beam pulse due to the absorption and multiple scattering. In [4], the impact of spatial spreading and temporal dispersion of an optical beam on an underwater optical link is investigated, and the spatial beam spreading may exert a more significant impact on temporal dispersion for the diffuse source than for the collimated source.

Many researchers have adopted Monte Carlo method to model the impulse response of the UWOC links. In [5–7], the authors adopt Monte Carlo simulation based on Henyey-Greenstein (HG) phase function to model the channel impulse response and time dispersion in different sea water. A Monte Carlo model together with a semi-analytic model is presented to calculate the impulse response in a range of environmental seawater for a particular underwater laser communications system [7]. In [8, 9], the authors developed an analytic method to model the light scattering in water based on the radiation transfer theory.

In this paper, instead of using the HG phase function or the TTHG phase function, we make use of the experimentally measured data values of the scattering phase function from Petzold's measurement in turbid sea water [11] and calculate scattering angles via a new numerical method. Based on our study, a closed-form expression of the double Gamma functions is adopted to fit the channel impulse response obtained from the Monte Carlo simulations.

---

*Received 24 November 2016, Accepted 3 February 2017, Scheduled 17 February 2017*

\* Corresponding author: Feibiao Dong (feibiaodong@163.com).

The authors are with the Department of Aeronautics and Astronautics, University of Electronic Science and Technology of China, Chengdu 611731, China.

The remainder of this paper is organized as follows. In Section 2, we introduce the effect of seawater on propagation beam pulse and the basic rules of our Monte Carlo approach. In Section 3, a new numerical method is proposed to obtain the scattering angle based on the measured value of the particle phase function. In Section 4, the channel impulse responses obtained from the proposed Monte Carlo model are shown, and the temporal dispersion and path loss for the UWOC links are evaluated. Conclusions are given in Section 5.

## 2. CHANNEL CHARACTERISTICS AND MONTE CARLO SIMULATION

### 2.1. Channel Characteristics in Seawater

Absorption and scattering are the two main processes that affect the light propagation in water, and both depend on incident wavelength. Absorption is an irreversible process, which depends on the water's index of refraction. Transmission photons will lose their energy partly when interacting with water molecule and other particles suspended in water. Scattering process leads to the deflection of optical beam from its original path because of the presence of the suspended particles of size comparable to the incident wavelength or the presence of some matters with different refraction index. We use the extinction coefficient  $k(\lambda) = k_a(\lambda) + k_s(\lambda)$  to characterize the total effects of absorption and scattering on light energy loss, here  $k_a(\lambda)$  and  $k_s(\lambda)$  represent the spectra absorption and scattering coefficient, respectively. The corresponding model parameters in turbid sea environment are summarized in Table 1 [12]. The scattering coefficient  $k_s^{Ray}$  is  $2.33 \times 10^{-3} \text{ m}^{-1}$  for blue/green light.

**Table 1.** Parameters for 532 nm laser in coastal and harbor water.

Water type	$k_a$ ( $\text{m}^{-1}$ )	$k_s$ ( $\text{m}^{-1}$ )	$k$ ( $\text{m}^{-1}$ )
Coastal	0.088	0.216	0.305
Harbor	0.295	1.875	2.170

### 2.2. Monte Carlo Simulation

Monte Carlo method based on radiation transfer equation (RTE) has been applied to light transmission problems in random media [13–15] by generating a large number of source photons according to the emitted light intensity distribution. It can simulate and track the absorption and scattering of each emitted photon interacted with the medium, and the channel characteristics can be evaluated by the impulse response. Monte Carlo approach is a more flexible method of studying light transport in dispersion medium compared with solving the RTE analytically. The basic rules of Monte Carlo approach are summarized as follows: photon position in Cartesian coordinates  $(x, y, z)$ ; the direction of transmission direction described by zenith angle  $\theta$  and azimuth angle  $\phi$ ; propagation time  $t$  and weight  $w$ ; each photon's position is initialized at  $(0, 0, 0)$  with zero start time and unit weight; the initial movement direction is calculated according to the divergence angle and angular intensity distribution of the source [19, 20].

Before interacting with the particle, the photon's propagation distance  $l$  can be calculated by  $l = \frac{-\ln \xi}{k_a + k_s}$ , here,  $\xi$  is a uniform random variable between 0 and 1, and the photon weight will be updated by  $w' = w \left(1 - \frac{k_s}{k_s + k_a}\right)$ . After scattering from the direction  $(\mu_x, \mu_y, \mu_z)$ , the next movement direction  $(\mu'_x, \mu'_y, \mu'_z)$  is determined by the zenith angle  $\theta$  and azimuth angle  $\phi = 2\pi\xi$ , then the new direction  $(\mu'_x, \mu'_y, \mu'_z)$  is specified by [16].

$$\begin{aligned}
 \mu'_x &= \frac{\sin \theta}{\sqrt{1 - \mu_z^2}} (\mu_x \mu_z \cos \phi - \mu_y \sin \phi) + \mu_x \cos \theta \\
 \mu'_y &= \frac{\sin \theta}{\sqrt{1 - \mu_z^2}} (\mu_y \mu_z \cos \phi + \mu_x \sin \phi) + \mu_y \cos \theta \\
 \mu'_z &= -\sin \theta \cos \phi \sqrt{1 - \mu_z^2} + \mu_z \cos \theta
 \end{aligned} \tag{1}$$

if the angle is too close to the  $z$ -axis (say  $|\mu_z| > 0.99999$ ), Eq. (1) does not make sense. Need to calculate as follows

$$\begin{aligned}\mu'_x &= \sin \theta \cos \phi \\ \mu'_y &= \sin \theta \sin \phi \\ \mu'_z &= \frac{\mu_z}{|\mu_z|} \cos \phi\end{aligned}\quad (2)$$

then, the new photon's location can be updated by

$$\begin{aligned}x' &= x + \mu'_x l \\ y' &= y + \mu'_y l \\ z' &= z + \mu'_z l\end{aligned}\quad (3)$$

The tracking should be terminated, when the photon reaches the receiver plane perpendicular to the  $z$  axis, or the photon's weight is lower than a threshold value of  $10^{-6}$ , and only the ones within the receiver aperture and with zenith angles less than the receiver FOV's half angle can be selected as the received photons. Repeatedly track until the last photon tracking is completed. The travel time, position, direction and weight for each photon are recorded. The accumulated weight of the detected photons with the same arrival time is normalized by the total transmit weight, which is used to present the curve of received intensity versus travel time for unit transmit intensity, and it is equivalent to the channel impulse response.

### 3. NUMERICAL SOLUTION FOR THE COMPUTING OF THE SCATTERING ANGLE

#### 3.1. Scattering Phase Function

To model the characterization of multiple scattering, the scattering phase function  $P(\theta, \lambda)$  is introduced to calculate the energy distribution characteristics of the scattered optical beam in certain directions. Integrating the  $P(\theta, \lambda)$  over all directions

$$1 = 2\pi \int_0^\pi P(\theta, \lambda) \sin \theta d\theta \quad (4)$$

where  $\theta$  is the angle of new propagation direction with respect to that of the current one.

After sampling for the phase function  $P(\theta)$ , the scattering angle can be computed by

$$\xi = 2\pi \int_0^{\theta_s} P(\theta) \sin \theta d\theta \quad (5)$$

where  $\xi$  is uniformly distributed between 0 and 1, and  $\theta_s$  is the scattering angle.

The HG function is widely used to represent the Mie scattering phase function with the expression as

$$P_{\text{HG}}(\theta) = \frac{1 - g^2}{4\pi (1 + g^2 - 2g \cos \theta)^{\frac{3}{2}}} \quad (6)$$

Here  $\theta$  is scattering angle, and  $g$  is the particle asymmetry factor. After sampling, the scattering angle becomes

$$\theta = \arg \cos \left\{ \frac{1}{2g} \left[ (1 + g^2) - \left( \frac{1 - g^2}{1 - g + 2g\xi} \right)^2 \right] \right\} \quad (7)$$

Here, the azimuth angle  $\varphi$  is uniformly distributed between 0 and  $2\pi$ , namely  $\varphi = 2\pi\xi$ .

In order to facilitate the calculation in the Monte Carlo simulations, the HG phase function is widely used to represent the scattering phase function. However, the HG function cannot match very well with Petzold's measurement of seawater scattering phase function in all ranges of angles. Thus, we adopt the Petzold's measured data values of the scattering phase function. To gain more data values of phase function, we employ Mobley's scheme [12] with linear interpolation for a particular angle range. Figure 1 presents the comparison between the HG function with  $g = 0.924$ .

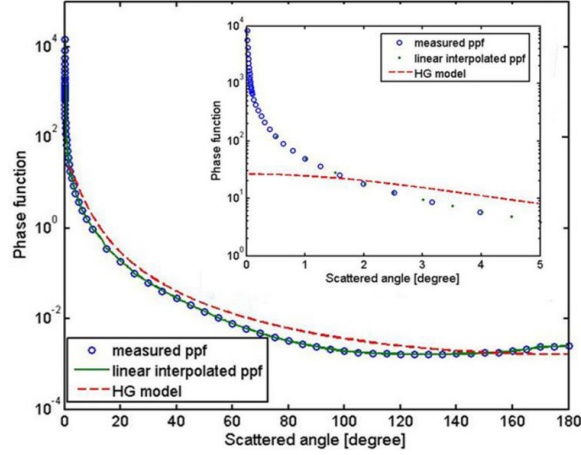


**Figure 1.** Particle phase function from [11] and HG phase function.

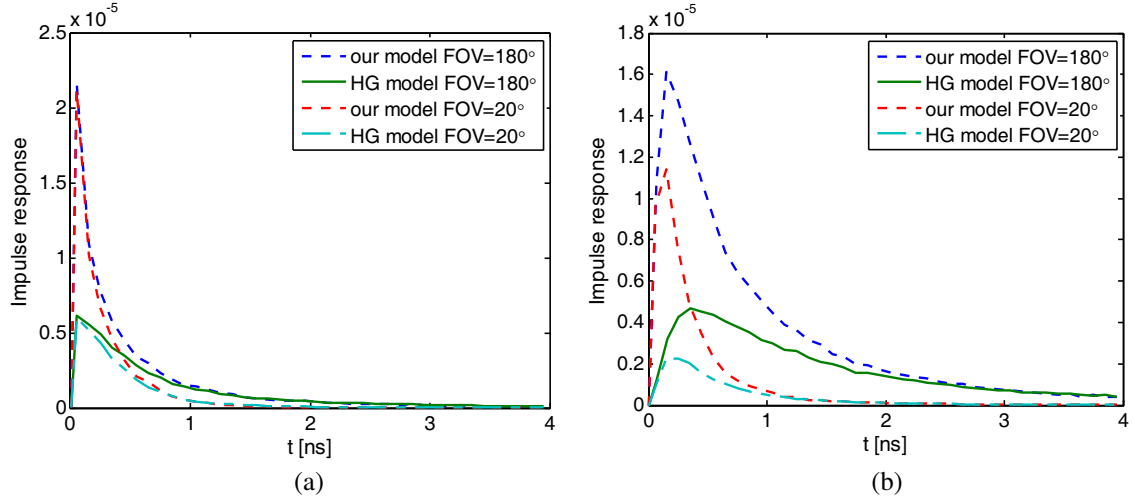


**Figure 2.** Impulse response by Monte Carlo (MC) simulation based on Petzold's measured phase function (our model) and HG phase function (HG model) respectively. (a) Coastal water ( $L = 30$  m). (b) Harbor water ( $L = 9$  m).

### 3.2. Numerical Method for The Computing of The Scattering Angle

In [19], the authors firstly adopted Petzold's measurement in the Monte Carlo simulation and presented the difference between the measured particle phase function and the HG phase function. However, the authors neither provided the numerical method used to obtain the scattering angle  $\theta_s$  by solving Eq. (5) nor illustrated the difference of effect on the impulse response between the Petzold's measurement and HG phase function in the turbid sea environment. Due to the processing of the Petzold's measured discrete data values of the phase function, it is difficult to obtain the  $\theta_s$  by solving Eq. (5). We propose a numerical solution for  $\theta_s$  of Eq. (5) to obtain the correspondence between the scattering angle and the random number. The steps are as follows:

(1). We take  $N$  discrete uniform points in the interval of  $[0, \pi]$ , and  $m$  is an integer from 1 to  $N$ . The scattering phase function derived from Petzold's measurement represents the total phase function  $P(\theta)$  at these discrete points. We normalize these discrete values, that is to satisfy the normalization condition as:

$$2\pi \sum_{m=1}^{m=N} P_m(\theta_m) \sin \theta_m \Delta\theta_m = 1$$

(2). For a specific scattering angle  $\theta_i$ , where  $i$  is an integer from 1 to  $N$ , the right-hand side of Eq. (5) can be calculated by

$$s_i = 2\pi \sum_{m=1}^{m=i} P_m(\theta_m) \sin \theta_m \Delta\theta_m$$

(3). Therefore, giving a uniformly distributed random variable  $\xi_i$  between 0 and 1, if its value satisfies the condition  $s_{i-1} < \xi_i \leq s_i$ , the scattering angle can be chosen as the scattering angle  $\theta_i$ .

To illustrate the difference of effect on temporal dispersion between the Petzold’s measurement and HG phase function, some Monte Carlo simulations were carried out. Figure 2 shows the channel impulse response obtained from Monte Carlo simulations based on Petzold’s measurement (adopted in our simulation model) and HG phase function, respectively. The results of the impulse response for different sea water link range scales  $L$  and FOVs are presented. Comparing our models with HG models, it can be seen that the difference of the channel impulse response is obvious, when using the two kinds of phase functions. The energy loss of the light propagation in turbid water is significantly larger than that of the HG phase function model. We can conclude that it is not appropriate to use HG phase function to model the channel impulse response in turbid sea water.

#### 4. SIMULATION RESULTS AND DISCUSSION

The proposed numerical method was applied in the Monte Carlo simulation. We consider a  $\lambda = 532$  nm source with maximum initial divergence angle  $\theta_0 = 10^\circ$  and a photon receiver with 50 cm aperture [10]. The double Gamma function is adopted to fit the channel impulse response obtained from the Monte Carlo simulations. The double Gamma function [17–19] is given by

$$h(t) = a(t - t_0) e^{-b(t-t_0)} + c(t - t_0) e^{-d(t-t_0)}, \quad t \geq t_0 \tag{8}$$

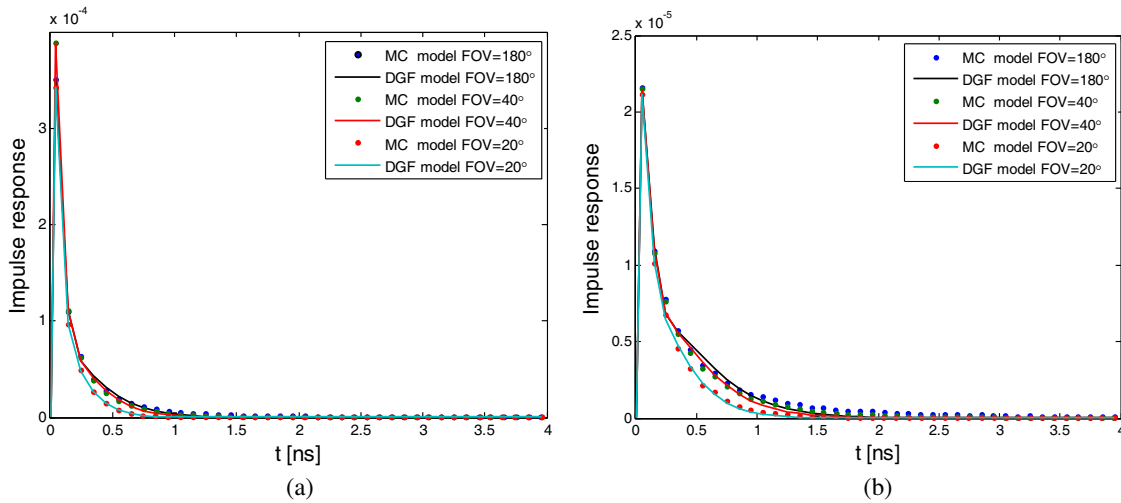


**Figure 3.** Impulse response in coastal water by Monte Carlo (MC) simulation and Double Gamma Functions (DGF) fitting. (a)  $L = 20$  m, (b)  $L = 30$  m.

**Table 2.** Time dispersion for various link ranges and FOVs in coastal and harbor.

Coastal			Harbor		
FOV	$L = 20$ m	$L = 30$ m	FOV	$L = 9$ m	$L = 12$ m
20°	0.615 ns	1.033 ns	20°	1.80 ns	4.30 ns
40°	0.824 ns	1.403 ns	40°	2.43 ns	5.55 ns
180°	0.936 ns	1.552 ns	180°	3.86 ns	7.90 ns

where  $a, b, c, d$  are the four parameters to be solved.  $t$  is the propagation time,  $L$  the link range scale,  $v$  the light speed in water, and  $t_0 = L/v$ . The parameter set  $(a, b, c, d)$  in Eq. (8) can be calculated from Monte Carlo simulation results via a nonlinear least square criterion as

$$(a, b, c, d) = \arg \min \left( \int [h(t) - h_{mc}(t)]^2 dt \right) \quad (9)$$

where  $h_{mc}(t)$  is obtained from the Monte Carlo simulation results, and  $h(t)$  is the double Gamma functions model in Eq. (8).  $\arg \min (\cdot)$  is the operator to return the parameter of the minimum.

Figures 3 and 4 illustrate the simulated impulse response obtained from the Monte Carlo simulations and the double Gamma functions fitting. The starting time of the impulse response is shifted from  $t_0$  to 0. The temporal dispersions (unit: nanosecond) calculated similarly for various water types, links ranges  $L$  and FOVs are shown in Table 2. With the increase of total attenuation, the photons may suffer more scattering, which leads to time dispersing more heavily. Wide FOV means wide configuration systems, and the photons suffering more multiple scattering can still be captured by the photon detector.

To characterize the attenuation of light propagation in the turbid sea water, Figure 5 illustrates the curve of path loss for different link ranges. We can find that the FOV's effects on the path loss in the

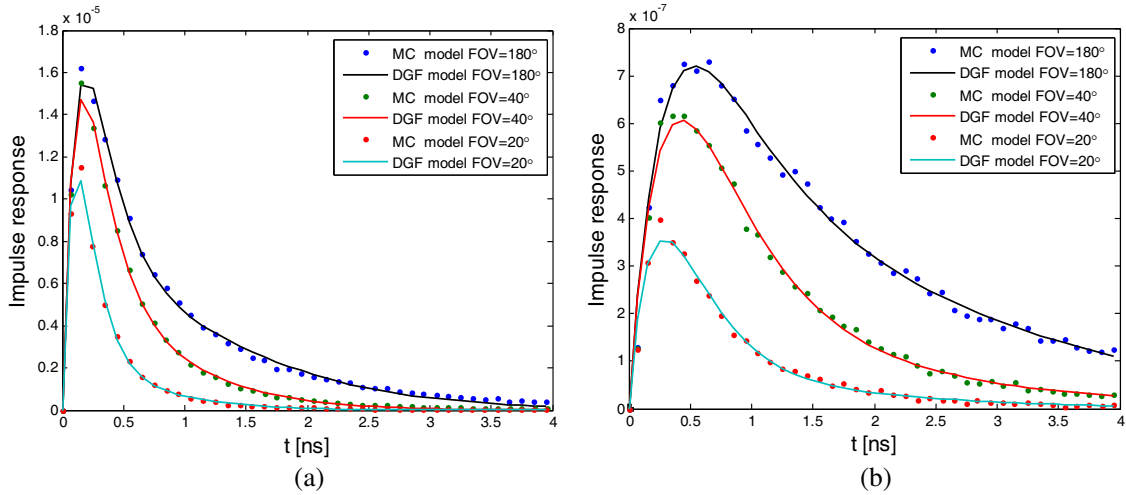


**Figure 4.** Impulse response in harbor water by Monte Carlo (MC) simulation and Double Gamma Functions (DGF) fitting. (a)  $L = 9$  m, (b)  $L = 12$  m.

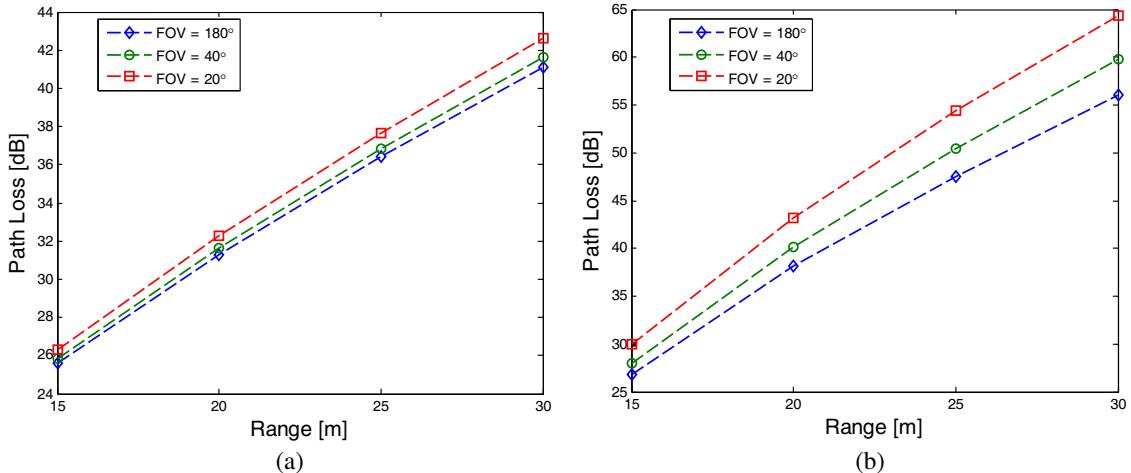


**Figure 5.** Curve of path loss for different link ranges. (a) Coastal water. (b) Harbor water.

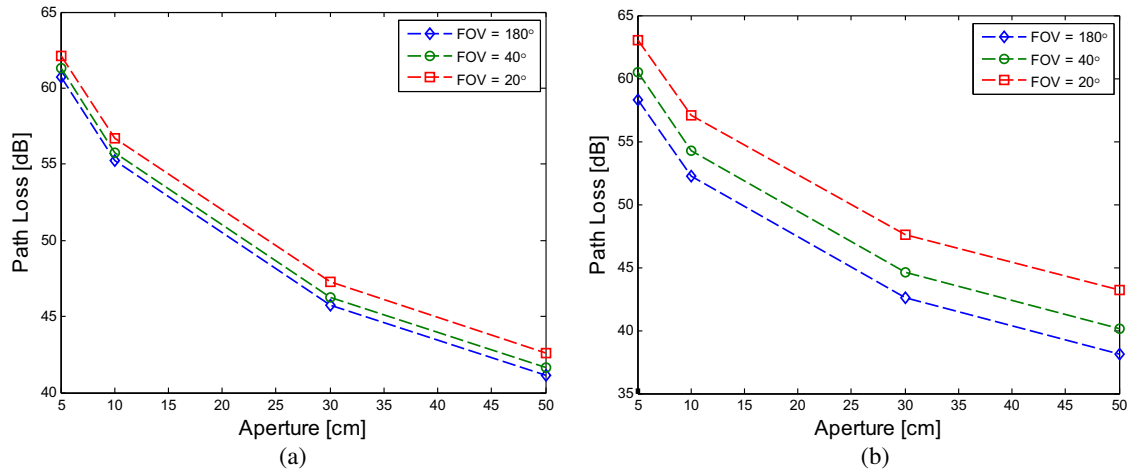


**Figure 6.** Curve of path loss for different apertures. (a) Coastal water ( $L = 30$  m). (b) Harbor water ( $L = 9$  m).

harbor water are larger than those in the coastal one. Figure 6 shows the quantitative dependence of the path loss on the receiver aperture size for both the coastal and harbor waters, in which the receiver aperture sizes change from 5 cm to 50 cm.

## 5. CONCLUSION

In this paper, we investigate the channel impulse response of the UWOC links in turbid seawater using the Monte Carlo approach. Through the numerical results, we show that the HG phase function cannot model the impulse response exactly in the turbid sea environment. Numerical results suggest that the temporal dispersion of the optical channels in turbid seawater is not negligible, and the receiving system parameters affect more heavily on the path loss in harbor water than in coastal water. The obtained impulse response is fitted well by the double Gamma function, which provides an alternative way to evaluate the UWOC system performance.

## ACKNOWLEDGMENT

This work was supported in part by the National Natural Science Foundation of China under Grant 61301261 and in part by the the National Nature Science Foundation of China under Grant G0504740161271286.

## REFERENCES

1. Giles, J. W. and I. Bankman, "Underwater optical communications systems. Part 2: Basic design considerations," *IEEE Military Communication Conf. (MILCOM)*, 1700–1705, Atlantic City, NJ, Oct. 3, 2005.
2. Anguita, D., D. Brizzolara, and G. Parodi, "Building an underwater wireless sensor network based on optical communication: Research challenges and current results," *Int. Conf. On Sensor Technologies and Applications (SENSORCOMM)*, 476–479, Athens Gree, Aug. 2009.
3. Zhang, H. and Y. Dong, "Impulse response modeling for general underwater wireless optical MIMO links," *IEEE Communications Magazine*, Vol. 54, No. 2, 56–61, 2016.
4. Cohenour, B. M. and L. J. Mullen, "Channel response measurements for diffuse non-line-sight (NLOS) optical communication links underwater," *Proc. 2011 IEEE Oceans Conf.*, 1–5, 2011.

5. Gabriel, C., M. Khalighi, S. Bourenane, P. Leon, and V. Rigaud, "Channel modeling for underwater optical communication," *Proc. 2011 IEEE Workshop on Optical Wireless Communication, Globecom Conf.*, 833–837, 2011.
6. Liang, B., H. Zhu, and W. Chen, "Simulation of laser communication channel from atmosphere to ocean," *ACTA Optical Sinica*, Vol. 27, No. 2, 0253–2239, 2007.
7. Dalgeish, F., F. Caimi, and A. Vuorenkoski, "Efficient laser pulse dispersion codes for turbid undersea imaging and communications applications," *Proc. of SPIE*, Vol. 7678, 1–12, 2010.
8. Jaruwatanadilok, S., "Underwater wireless optical communication channel modeling and performance evaluation using vector radiative transfer theory," *IEEE Journal on Selected Areas in Communications*, Vol. 26, No. 9, 1620–1627, 2008.
9. Hanson, F. and S. Radic, "High bandwidth underwater optical communication," *Appl. Opt.*, Vol. 47, No. 2, 277–283, 2008.
10. Gabriel, C., M. Khalighi, S. Bourenane, P. Leon, and V. Rigaud, "Monte-Carlo-based channel characterization for underwater optical communication systems," *J. Opt. Commun. Netw.*, Vol. 8, No. 1, 1–12, 2013.
11. Petzold, T., "Volume scattering functions for selected ocean waters," SIO Ref., Scripps Institution of Oceanography Visibility Laboratory, 70–78, San Diego, CA, 1972.
12. Mobley, C. D., *Light and Water: Radiative Transfer in Natural Waters*, Academic Press, 1994.
13. Li, J., Y. Ma, Q. Zhou, B. Zhou, and H. Wang, "Monte Carlo study on pulse response of underwater optical channel," *Optical Engineering*, Vol. 51, No. 6, 1–5, 2012.
14. Winker, D. M. and L. R. Poole, "Monte Carlo calculation of cloud returns for ground-based and space-based lidars," *APPI. Phy. B*, Vol. 60, No. 4, 341–344, 1995.
15. Yang, C. C. and K. C. Yeh, "Scattering from a multiple-layered random medium," *J. Opt. Soc. Am.*, Vol. 2, No. 12, 2112–2119, 1985.
16. Pral, S. A., M. Keijzer, and S. L. Jacques, "A Monte Carlo of light propagation in tissue," *SPIE Proceedings*, Vol. 5, 102–111, 1989.
17. Mooradian, G. and M. Celler, "Temporal and angular spreading of bluegreen pulses in clouds," *Applied Optics*, Vol. 21, No. 9, 1572–1577, 1982.
18. Tang, S., Y. Dong, and X. Zhang, "On impulse response modeling for underwater wireless optical links," *Proc. 2013 IEEE/MTS Ocean Conf.*, 1–4, 2013.
19. Tang, S., Y. Dong, and X. Zhang, "Impulse response modeling for underwater wireless optical communication links," *IEEE Trans. Commun.*, Vol. 62, No. 1, 226–234, 2014.
20. Ding, H., G. Chen, A. Majumdar, B. Sadler, and Z. Xu, "Modeling of non-line-of-sight ultraviolet scattering channels for communication," *IEEE J. Sel. Areas Commun.*, Vol. 27, No. 9, 1535–1544, 2009.